



Thermoelectromechanical instability of dielectric elastomer undergoes polarization saturation and temperature variation

Yaguang Guo¹ · Liwu Liu¹ · Yanju Liu¹ · Jinsong Leng²

Received: 29 September 2020 / Revised: 4 November 2020 / Accepted: 17 November 2020 / Published online: 2 April 2021
© The Chinese Society of Theoretical and Applied Mechanics and Springer-Verlag GmbH Germany, part of Springer Nature 2021

Abstract

When the electric field caused by voltage reaches a certain level, the charge on the compliant electrodes will not increase owing to the polarization saturation, which would limit the deformation of the dielectric elastomer. Some experiments show that temperature also has a significant effect on the deformation of dielectric elastomer. In this work, a free energy model coupling temperature and polarization saturation is developed to characterize the thermoelectromechanical instability of dielectric elastomer. The results reveal that both the polarization saturation parameters and electric field have a significant influence on the actuation ability of the dielectric elastomer, and the increase of temperature enhances thermoelectromechanical stability. It is hoped that this work could guide the development of dielectric elastomer materials and application devices operating in variable temperatures.

Keywords Dielectric elastomer · Thermoelectromechanical instability · Polarization saturation · Temperature variation

1 Introduction

In recent years, soft materials such as shape memory polymers, hydrogels, electroactive polymers, etc. have received much attention [1–5]. As a typical electroactive material, dielectric elastomer (DE) can generate large deformation under an external electric field [6]. Dielectric elastomer has excellent characteristics, such as fast response speed, light weight, and high elastic energy density, etc., and has been widely used to design diverse applications, including actuators, energy harvester, sensors, soft robots, optical devices [7–14].

When the dielectric elastomer actuator deforms, the mechanical force and external electric field have a significant influence on its performance. Dielectric elastomer membrane would expand its area and contract its thickness under

an external electric field. Such changes will cause positive feedback, creating a very high electric field between the two compliant electrodes. The membrane will be breakdown by electric field once the value exceeds the breakdown strength of the material. This failure is known as electromechanical instability, which greatly limits the application of dielectric elastomer actuator [15]. For ideal dielectric elastomer, a general method was developed to analyze the electromechanical stability. The calculation results show that the pre-stretch suppresses electromechanical instability and enhances actuation ability, agreeing well with experimental results [16]. The electromechanical instability has also been analyzed in detail based on this method when dielectric elastomer actuator generates homogeneous in-plane and inhomogeneous out-of-plane large deformations [17, 18]. Generally, the dielectric elastomer is considered as linear dielectrics. However, dielectric elastomer will experience polarization saturation when it deforms under an external electric field. A model was proposed to analyze the effect of polarization saturation of dipoles on the snap-through instability [19]. Considering the hyperelastic and nonlinear dielectric behavior, a thermodynamic model was also developed to investigate the instability of the dielectric elastomer when polarization saturation occurs [20].

Few of the existing studies have considered the impact of temperature changes on the properties of dielectric

Executive Editor: Xi-Qiao Feng

✉ Liwu Liu
liulw@hit.edu.cn

✉ Jinsong Leng
lengjs@hit.edu.cn

¹ Department of Astronautical Science and Mechanics, Harbin Institute of Technology, Harbin 150001, China

² Center for Composite Materials and Structures, Science Park of Harbin Institute of Technology, Harbin 150080, China

elastomer. It has been reported that the Young’s modulus of the commercial acrylic elastomer (VHB 4910, 3M, USA) has a strong dependence on temperature [21], and the dielectric constant of the material is also related to the stretch and temperature [22]. For acrylic dielectric elastomer materials (VHB 4910), the relationship between dielectric constant and temperature has been studied experimentally in detail. A model was also developed based on experimental results [23]. Further, the thermal effects on the electromechanical instability and nonlinear dynamic behavior of dielectric elastomer were investigated [24, 25]. The thermoelectromechanical instability of dielectric elastomer by considering the dependence of dielectric constant on temperature and deformation was also investigated [26, 27].

In this work, different from previous studies which only considered the influence of temperature or polarization saturation on the instability of dielectric elastomer, we concentrate on the impact of temperature variation on thermoelectromechanical instability of dielectric elastomer when they experience polarization saturation under the action of an external electric field. Following the previous studies [24, 26–28], a free energy model, including thermoelastic strain energy and electric energy is derived. When the temperature changes, the thermal contribution is taken into account in the thermoelastic strain energy. The nonlinear dielectric behavior and the temperature-dependent dielectric constant are considered when establishing the free energy model of electric field energy. In this way, the thermoelectromechanical instability of the dielectric elastomer is characterized in detail by the specific model.

2 Free energy model

As illustrated in Fig. 1, for a general dielectric elastomer actuator, both surfaces of the membrane are coated with compliant electrodes. In reference state, the temperature of the environment is T_0 , and the dimensions along three

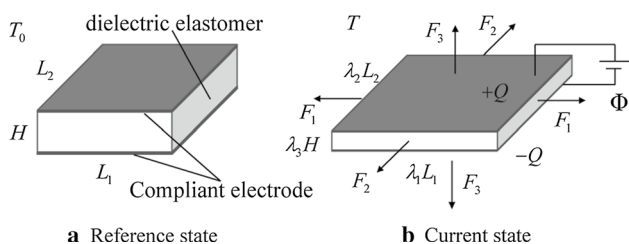


Fig. 1 Deformation principle of a general dielectric elastomer actuator. **a** In reference state, the temperature of the environment is T_0 , and the dielectric elastomer membrane is undeformed with no voltage and mechanical force. **b** In current state, the ambient temperature becomes T , and the dielectric elastomer membrane deforms by mechanical forces and voltage

principal directions of the membrane in the absence of mechanical force and electric field are L_1 , L_2 , and H . In current state, the ambient temperature becomes T , and the dimensions of the membrane change into $\lambda_1 L_1$, $\lambda_2 L_2$, and $\lambda_3 H$ with the applied mechanical forces along three principal directions F_1 , F_2 , and F_3 , voltage Φ on the two compliant electrodes, where λ_1 , λ_2 , and λ_3 are stretches along with three principal directions. Electric charges Q are accumulated on the two electrodes respectively, while the entropy is S . Define the nominal stresses by $\sigma_1^{\sim} = F_1/(L_2 H)$, $\sigma_2^{\sim} = F_2/(L_1 H)$, and $\sigma_3^{\sim} = F_3/(L_1 L_2)$, nominal electric displacement by $D^{\sim} = Q/(L_1 L_2)$, nominal electric field by $E^{\sim} = \Phi/H$, and nominal entropy by $s^{\sim} = S/(L_1 L_2 H)$.

The thermodynamic system is composed of dielectric elastomer, voltage, mechanical forces, and temperature. The free energy function of the thermodynamic system depends on five independent variables [20]

$$W(\lambda_1, \lambda_2, \lambda_3, D^{\sim}, T) = W_s(\lambda_1, \lambda_2, \lambda_3, T) + W_e(\lambda_1, \lambda_2, \lambda_3, D^{\sim}, T), \tag{1}$$

where $W_s(\lambda_1, \lambda_2, \lambda_3, T)$ and $W_e(\lambda_1, \lambda_2, \lambda_3, D^{\sim}, T)$ represent the thermoelastic strain energy and electric field energy of the dielectric elastomer, respectively. When the thermodynamic system is in equilibrium in the current state, the Eq. (1) should be minimized. Follow the previous studies [28], we can get the state equations by the partial derivation of the free energy density function

$$\sigma_1^{\sim} = \frac{\partial W(\lambda_1, \lambda_2, \lambda_3, D^{\sim}, T)}{\partial \lambda_1}, \tag{2}$$

$$\sigma_2^{\sim} = \frac{\partial W(\lambda_1, \lambda_2, \lambda_3, D^{\sim}, T)}{\partial \lambda_2}, \tag{3}$$

$$\sigma_3^{\sim} = \frac{\partial W(\lambda_1, \lambda_2, \lambda_3, D^{\sim}, T)}{\partial \lambda_3}, \tag{4}$$

$$E^{\sim} = \frac{\partial W(\lambda_1, \lambda_2, \lambda_3, D^{\sim}, T)}{\partial D^{\sim}}, \tag{5}$$

$$s^{\sim} = -\frac{\partial W(\lambda_1, \lambda_2, \lambda_3, D^{\sim}, T)}{\partial T}. \tag{6}$$

In an elastomer, each individual polymer chain has a finite contour length. The polymer chains are coiled allowing a large number of conformations when the elastomer subjected to no loads. The polymer chains become less coiled when subjected to loads. When the end-to-end distance of each polymer chain approaches the finite contour length with the increase of loads, the elastomer approaches the limiting stretch and stiffens steeply. This effect is absent in the

Neo–Hookean model, but represented by Gent [29] model. In the temperature field, the thermoelastic strain energy density function is [30]

$$W_s(\lambda_1, \lambda_2, \lambda_3, T) = \frac{T}{T_0} \left[-\frac{\mu J_{\text{lim}}}{2} \log \left(1 - \frac{\lambda_1^2 + \lambda_2^2 + \lambda_3^2 - 3}{J_{\text{lim}}} \right) \right] + c_0 [(T - T_0) - T \log (T/T_0)], \tag{7}$$

where μ is the shear modulus, $J_{\text{lim}} = \lambda_{1\text{lim}}^2 + \lambda_{2\text{lim}}^2 + \lambda_{3\text{lim}}^2 - 3$ is a constant reflecting the stretch limit of the material, and c_0 is a material parameter of polar dielectric. The stretches are restricted as $0 \leq (\lambda_1^2 + \lambda_2^2 + \lambda_3^2 - 3)/J_{\text{lim}} < 1$. When stretches are small, $(\lambda_1^2 + \lambda_2^2 + \lambda_3^2 - 3)/J_{\text{lim}} \rightarrow 0$, the Gent model recovers the Neo-Hookean model. When the stretches approach the limit, $(\lambda_1^2 + \lambda_2^2 + \lambda_3^2 - 3)/J_{\text{lim}} \rightarrow 1$, the Gent model stiffens steeply. The two items on the right side of Eq. (7) are the Gent thermoelastic strain energy and thermal contribution.

The appearance of electric field will polarize dielectric materials [28]. The electric displacement is small and increases linearly when the dielectric elastomer in a relatively weak electric field. In the case of electric field increases to a certain level, all the dipoles in the dielectric material will rotate in the same direction as the electric field and aligned perfectly. The electric displacement reaches saturation D_s and no longer increases with electric field [20], seen in Fig. 2. As an idealization, when polarization saturation occurs under the action of electric field, the nonlinear function of true electric field is [19, 31]

$$E = f(D) = \frac{D_s}{2\epsilon} \log \left(\frac{1 + D/D_s}{1 - D/D_s} \right), \tag{8}$$

where ϵ is the permittivity. Generally, dielectric elastomer is idealized, and the permittivity is regarded as a constant

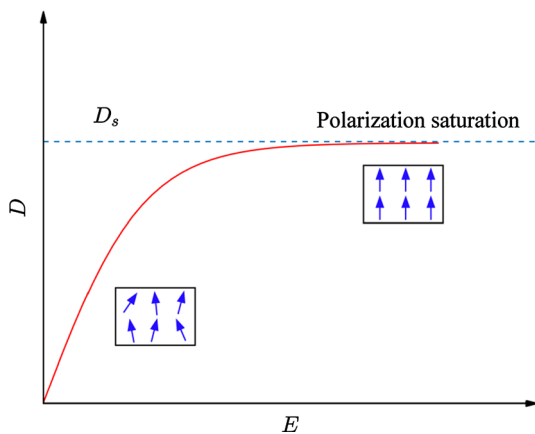


Fig. 2 Polarization curve of the dielectric material [20]. The curve can be regarded as linear at a weak electric field, and tends to a constant value when the electric field is sufficiently high

independent of any independent variable. However, a change in ambient temperature will also cause a change in the permittivity. Under the temperature field, the permittivity of the dielectric material can be written as $\epsilon = \epsilon_0 \epsilon_r(T)$, where $\epsilon_0 = 8.85 \times 10^{-12}$ F/m is the permittivity of the vacuum. The temperature dependent dielectric constant $\epsilon_r(T)$ can be described as [23]

$$\epsilon_r(T) = 2.18 + \frac{740}{T}. \tag{9}$$

Considering two pairs of work conjugate parameters, the relationship between nominal quantity and true quantity are $D^\sim = D\lambda_1\lambda_2$ and $E^\sim = E\lambda_3$, respectively. The electric energy density can be rewritten as

$$W_e(\lambda_1, \lambda_2, \lambda_3, D^\sim, T) = \int_0^{D^\sim} E^\sim dD^\sim = \lambda_3 \int_0^{D^\sim} f(D^\sim \lambda_1^{-1} \lambda_2^{-1}) dD^\sim. \tag{10}$$

According to Eqs. (8)–(10), we can get the special electric energy undergoing polarization saturation and temperature variation

$$W_e(\lambda_1, \lambda_2, \lambda_3, D^\sim, T) = \frac{D^\sim D_s \lambda_3}{2\epsilon_0(2.18 + 740/T)} \log \left(\frac{-D^\sim + D_s \lambda_1 \lambda_2}{D^\sim - D_s \lambda_1 \lambda_2} \right) + \frac{D_s^2 \lambda_1 \lambda_2 \lambda_3}{2\epsilon_0(2.18 + 740/T)} \log \left(1 - \frac{D^\sim \lambda_1^{-2} \lambda_2^{-2}}{D_s^2} \right). \tag{11}$$

Here, the dielectric elastomer is subjected to equal-biaxial forces $F_1 = F_2 = F$ and considered to be incompressible $\lambda_1 \lambda_2 \lambda_3 = 1$. Therefore, the stretches can be written as $\lambda_1 = \lambda_2 = \lambda$ and $\lambda_3 = \lambda^{-2}$. Then, substituting Eqs. (7) and (11) into Eq. (1) yields

$$W(\lambda, D^\sim, T) = \frac{T}{T_0} \left[-\frac{\mu J_{\text{lim}}}{2} \log \left(1 - \frac{2\lambda^2 + \lambda^{-4} - 3}{J_{\text{lim}}} \right) \right] + c_0 [(T - T_0) - T \log (T/T_0)] + \frac{D^\sim D_s \lambda^{-2}}{2\epsilon_0(2.18 + 740/T)} \log \left(\frac{-D^\sim + D_s \lambda^2}{D^\sim - D_s \lambda^2} \right) + \frac{D_s^2}{2\epsilon_0(2.18 + 740/T)} \log \left(1 - \frac{D^\sim{}^2}{D_s^2 \lambda^4} \right). \tag{12}$$

In the light of Eqs. (2)–(6) and Eq. (12), we can obtain

$$\sigma^\sim = \frac{T}{T_0} \left[-\frac{\mu J_{\text{lim}} (\lambda - \lambda^{-5})}{2\lambda^2 + \lambda^{-4} - J_{\text{lim}} - 3} \right] - \frac{D^\sim D_s \lambda^{-3}}{2\epsilon_0(2.18 + 740/T)} \log \left(\frac{-D^\sim + D_s \lambda^2}{D^\sim - D_s \lambda^2} \right), \tag{13}$$

$$E^\sim = \frac{D_s \lambda^{-2}}{2\epsilon_0(2.18 + 740/T)} \log \left(\frac{-D^\sim + D_s \lambda^2}{D^\sim - D_s \lambda^2} \right), \tag{14}$$

$$\begin{aligned}
 s^{\sim} = & -\frac{1}{T_0} \left[-\frac{\mu J_{\text{lim}}}{2} \log \left(1 - \frac{2\lambda^2 + \lambda^{-4} - 3}{J_{\text{lim}}} \right) \right] \\
 & + c_0 \log (T/T_0) - \frac{370}{\epsilon_0(2.18 + 740/T)^2 T^2} \\
 & \times \left[D^{\sim} D_s \lambda^{-2} \log \left(-\frac{D^{\sim} + D_s \lambda^2}{D^{\sim} - D_s \lambda^2} \right) + D_s^2 \log \left(1 - \frac{D^{\sim 2}}{D_s^2 \lambda^4} \right) \right].
 \end{aligned}
 \tag{15}$$

3 Thermoelectromechanical instability

The nominal electric displacement can be expressed as $D^{\sim} = \frac{\exp [2E^{\sim} \lambda^2 \epsilon_0(2.18+740/T)/D_s]-1}{\exp [2E^{\sim} \lambda^2 \epsilon_0(2.18+740/T)/D_s]+1} D_s \lambda^2$ on the basis of Eq. (14), and is substituted in Eqs. (13) and (15), we got the normalized stress and entropy

$$\begin{aligned}
 \frac{\sigma^{\sim}}{\mu} = & \frac{T}{T_0} \left[-\frac{J_{\text{lim}} (\lambda - \lambda^{-5})}{2\lambda^2 + \lambda^{-4} - J_{\text{lim}} - 3} \right] \\
 & - \frac{D_s}{\sqrt{\mu \epsilon_0}} \frac{E^{\sim}}{\sqrt{\mu/\epsilon_0}} \lambda \frac{\exp \left[2\lambda^2 \left(2.18 + \frac{740}{T} \right) \frac{E^{\sim}}{\sqrt{\mu/\epsilon_0}} / \frac{D_s}{\sqrt{\mu \epsilon_0}} \right] - 1}{\exp \left[2\lambda^2 \left(2.18 + \frac{740}{T} \right) \frac{E^{\sim}}{\sqrt{\mu/\epsilon_0}} / \frac{D_s}{\sqrt{\mu \epsilon_0}} \right] + 1},
 \end{aligned}
 \tag{16}$$

$$\begin{aligned}
 \frac{s^{\sim}}{\mu/T_0} = & \frac{J_{\text{lim}}}{2} \log \left(1 - \frac{2\lambda^2 + \lambda^{-4} - 3}{J_{\text{lim}}} \right) + \frac{c_0}{\mu/T_0} \log (T/T_0) \\
 & - \frac{740T_0}{(2.18 + 740/T)T^2} \frac{D_s}{\sqrt{\mu \epsilon_0}} \frac{E^{\sim}}{\sqrt{\mu/\epsilon_0}} \lambda^2 \frac{\exp \left[2\lambda^2 \left(2.18 + \frac{740}{T} \right) \frac{E^{\sim}}{\sqrt{\mu/\epsilon_0}} / \frac{D_s}{\sqrt{\mu \epsilon_0}} \right] - 1}{\exp \left[2\lambda^2 \left(2.18 + \frac{740}{T} \right) \frac{E^{\sim}}{\sqrt{\mu/\epsilon_0}} / \frac{D_s}{\sqrt{\mu \epsilon_0}} \right] + 1} \\
 & - \frac{370T_0}{\epsilon_0(2.18 + 740/T)^2 T^2} \frac{D_s^2}{\mu \epsilon_0} \log \left\{ 1 - \frac{\exp \left[2\lambda^2 \left(2.18 + \frac{740}{T} \right) \frac{E^{\sim}}{\sqrt{\mu/\epsilon_0}} / \frac{D_s}{\sqrt{\mu \epsilon_0}} \right] - 1}{\exp \left[2\lambda^2 \left(2.18 + \frac{740}{T} \right) \frac{E^{\sim}}{\sqrt{\mu/\epsilon_0}} / \frac{D_s}{\sqrt{\mu \epsilon_0}} \right] + 1} \right\}^2.
 \end{aligned}
 \tag{17}$$

In the following numerical study, representative parameters are selected, $T_0 = 293$ K, $c_0 = 1.7 \times 10^6$ J · km⁻³, $\mu = 45$ kPa, $J_{\text{lim}} = 120$ [27, 32, 33]. As illustrated in Fig. 3 are nominal stress-stretch curves under different values of nominal saturation electrical displacements and nominal electric fields, i.e. $D_s/\sqrt{\mu \epsilon_0}$ and $E^{\sim}/\sqrt{\mu/\epsilon_0}$. It is clear to see that all the curves coincide in Fig. 3a, and the nominal stress monotonically increases as the stretch increases in the absence of electric field. Comparing Fig. 3a–d, when the nominal saturated electric displacement value of the dielectric elastomer is relatively small, the nominal stress always increases monotonically with the increase

of stretch, even if the applied electric field is large. This phenomenon can be explained by the fact that the nominal electric displacement has been saturated under the action of a weak electric field. Thus, the increase of nominal electric field no longer causes the Maxwell stress to increase. If the value of the nominal saturation electric displacement of the dielectric elastomer is slightly larger, the nominal stress-stretch curves change from monotonously increasing to N-shaped, and can be lowered by the electric field. When the dielectric elastomer with an immense saturation electric displacement value and under a higher electric field, the nominal stress-stretch curve would be divided into two parts, Fig. 3c, d. It can be explained as follows: when subject to voltage, the Maxwell stress makes the dielectric elastomer membrane reduce its thickness; in turn, the reducing of thickness increases the Maxwell stress. Such a positive feedback tendency exists throughout the whole loading process. At a certain voltage, with the increase of stretch, the membrane reduce its thickness and the Maxwell stress is balanced by tensile stress. Once the stretch reaches a critical value, the process is motived, the Maxwell stress increases dramatically and exceeds the tensile stress when the nominal saturation electric displacement is not reached, resulting in the nominal stress less than zero. As the stretch approaches the limiting stretch,

the dielectric elastomer becomes stiffer, resulting in a sharp rise in tensile stress, and the curve goes up again.

Considering the effect of temperature, we set $D_s/\sqrt{\mu \epsilon_0} = 10$, and $E^{\sim}/\sqrt{\mu/\epsilon_0} = 0.12$. As can be seen from Fig. 4, as the temperature increases, the stress-stretch curve gradually changes from an N-shaped to monotonically increasing. The increase of temperature decreased the influence of Maxwell stress on tensile stress.

Figure 5 shows the variations of the nominal electric field with stretch under different nominal saturation electrical displacements when the temperature is $T = 293$ K. When saturated electric displacement is small, the dielectric elastomer

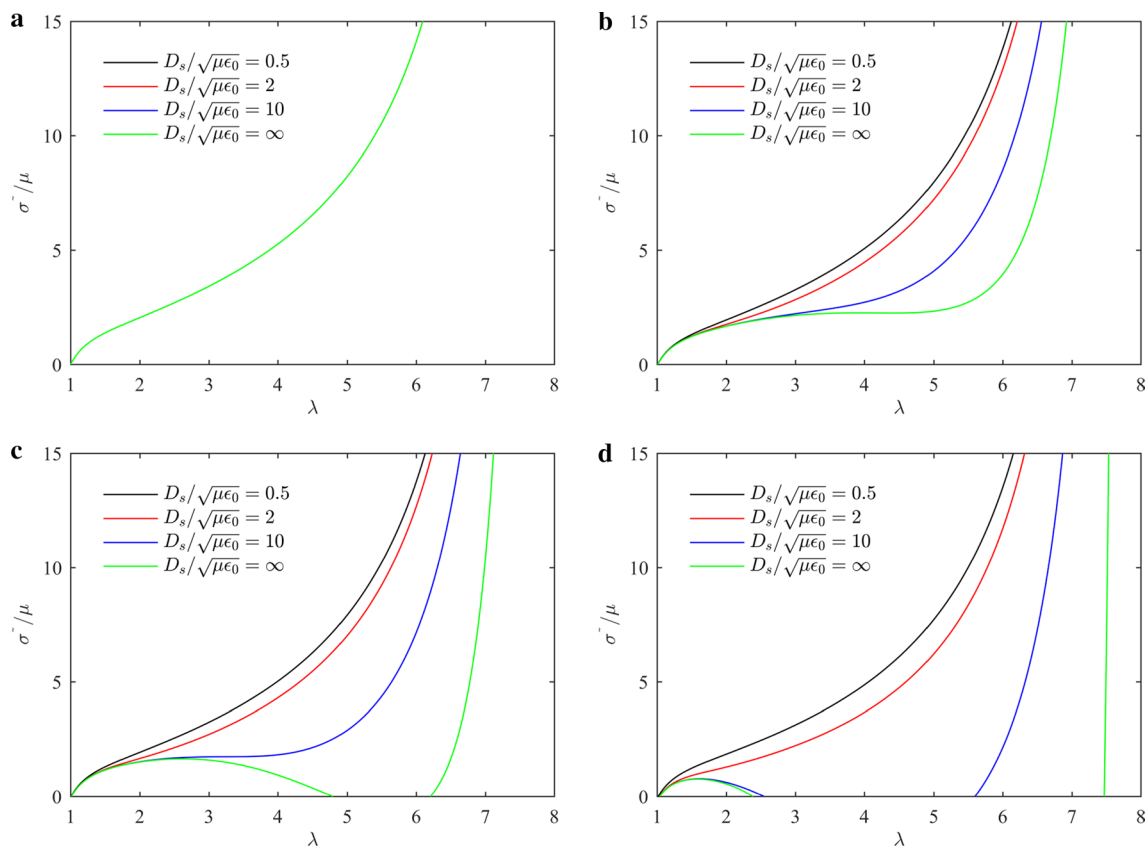


Fig. 3 Nominal stress-stretch curves under different saturated electric displacement when the nominal electric field are **a** $E^-/\sqrt{\mu/\epsilon_0} = 0$, **b** $E^-/\sqrt{\mu/\epsilon_0} = 0.1$, **c** $E^-/\sqrt{\mu/\epsilon_0} = 0.12$, and **d** $E^-/\sqrt{\mu/\epsilon_0} = 2$, respectively

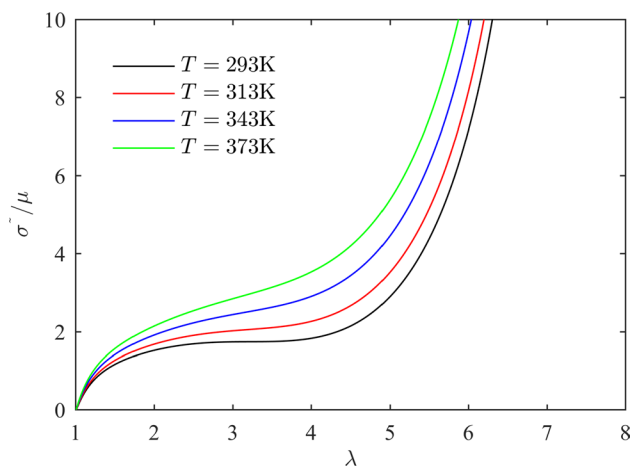


Fig. 4 Nominal stress-stretch curves under different temperatures membrane can only achieve a small actuation stretch even under a high electric field. With a larger value of the nominal saturation electric displacement, a more massive actuation stretch can be achieved with a smaller electric field, and the curve gradually changes from monotonous to a typical N-shaped, which may result in electromechanical instability or snap-through instability.

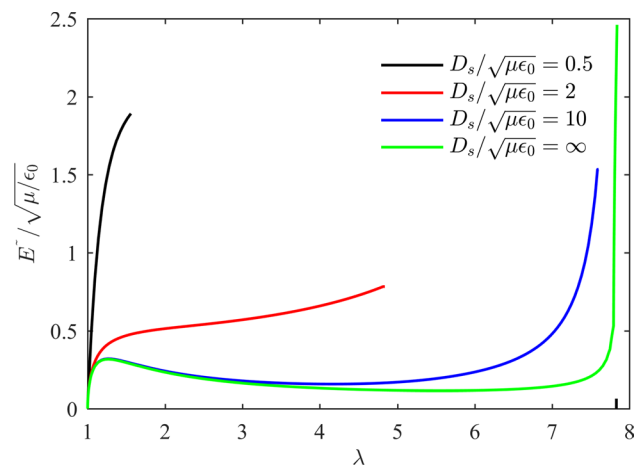


Fig. 5 Variations of the nominal electric field with stretch under different saturated electric displacements

Under the action of the electric field, electromechanical instability would induce dielectric elastomer actuator failure via electrical breakdown. Some experimental and theoretical studies show that the stability of the actuator is markedly enhanced by pre-stretch [6, 16, 31]. Considering the

polarization saturation, Fig. 6 illustrates the variations of the nominal electric field with stretch, where $D_s/\sqrt{\mu\epsilon_0} = 10$, and $T = 293$ K. Obviously, the curve gradually changes from N-shaped to monotonous increase as the pre-stretch increases. This means electromechanical instability is suppressed, and the actuation stretch is increased, which is consistent with the results of Zhao and Suo [16].

The effect of temperature on the nominal electric field-stretch curve is shown in Fig. 7. When electromechanical instability occurs, the critical electric field usually determines the electrical breakdown. Clearly, when the temperature rises, the critical value increases, which means that the thermoelectromechanical stability is improved. After thermoelectromechanical instability, the actuator may survive without electrical breakdown. With the further increase of stretch, the membrane becomes stiffer, which lead to the curve of the nominal electric field rises again. Hence, the dielectric elastomer membrane will suddenly change from a state with a small area to a state with a large area. This process is also known as snap-through instability. The red dashed line in Fig. 7 indicates the electrical breakdown, and the arrow indicates the snap-through process. If we assume that the membrane can just survive in the snap-through process at $T = 293$ K, as shown by the black arrow, the increase of critical value of the nominal electric field will lead to the snap-through occurs under a higher electric field when the temperature rises. Therefore, the membrane will suffer electrical breakdown at first and cannot survive in the snap-through, indicated by the green arrow.

Next, we analyze the effects of temperature and electric field on entropy. Variations of nominal entropy with the temperature and stretch are illustrated in Fig. 8. The nominal entropy increases gradually with the rise in temperature. When the stretch is small, the change of nominal entropy is almost negligible. According to the third law of thermodynamics, the

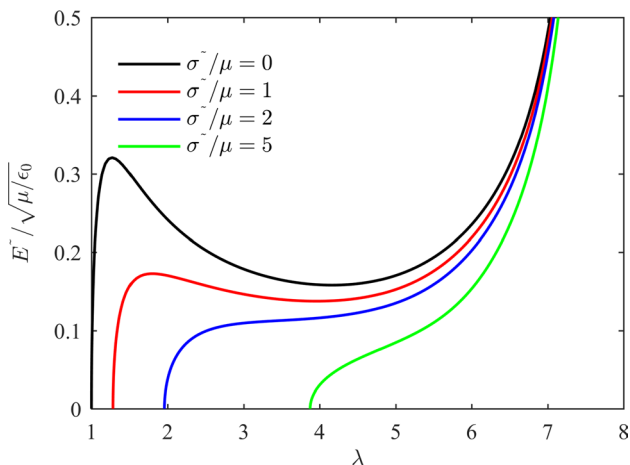


Fig. 6 Variations of the nominal electric field with stretch under different nominal stresses

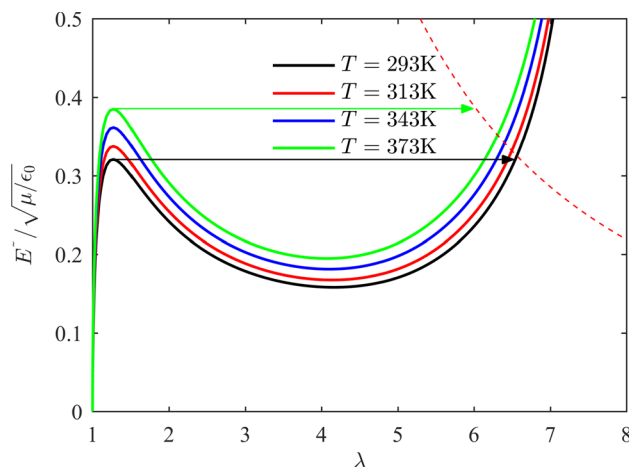


Fig. 7 Variations of the nominal electric field with stretch under different temperatures

increase of temperature causes entropy to increase so that the thermodynamic system will approach a more stabilized state. It is also noted that a significant decrease in nominal entropy occurs when the stretch limit is approached. The physical process can be explained as follows: as dielectric elastomer membrane is stretched in planar directions, the coiled chain will be elongated, and in a more orderly state, thus the entropy declines with the deformation. Figure 9 is a view of the effects of the applied stretch and electric field on entropy. When the nominal electric field rises, there is almost no change in the nominal entropy when the stretch is small. When the stretch is close to the stretch limit, the nominal entropy decreases as the increase of the stretch and nominal electric field.

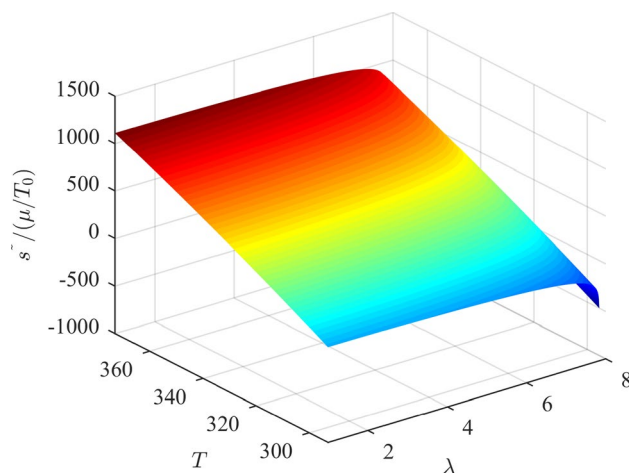


Fig. 8 Variations of nominal entropy with temperature and stretch

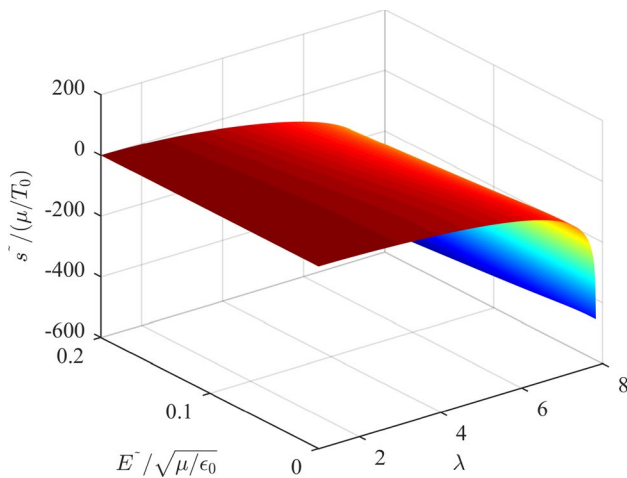


Fig. 9 Variations of nominal entropy with nominal electric field and stretch

4 Conclusion

In conclusion, a free energy model is derived based on the thermodynamics frame to characterize the effect of polarization saturation and temperature variation on the thermoelectromechanical instability of the dielectric elastomer. The numerical results indicate that the actuation ability of the dielectric elastomer is exceedingly affected by the electric field and polarization saturation parameter. The electromechanical instability can also be suppressed, and actuation stretch is increased by prestresses when dielectric elastomer actuator undergoes polarization saturation. With the increase of temperature, the thermoelectromechanical stability is strengthened. The temperature has a significant effect on entropy, while the impact of stretch and electric field can be almost ignored. It is hoped that this work can provide guidance in the design of high-performance dielectric elastomer materials and various dielectric elastomer application devices operating in variable temperatures.

Acknowledgements This work was supported by the National Natural Science Foundation of China (Grant 11772109).

References

- Shen, Z., Chen, F., Zhu, X., et al.: Stimuli-responsive functional materials for soft robotics. *J. Mater. Chem. B* **8**, 8972–8991 (2020)
- Li, H., Liang, X., Song, W.: Buckling-controlled two-way shape memory effect in a ring-shaped bilayer. *Acta Mech. Sin.* **35**, 1217–1225 (2019)
- White, T.J., Broer, D.J.: Programmable and adaptive mechanics with liquid crystal polymer networks and elastomers. *Nat. Mater.* **14**, 1087–1098 (2015)
- Wang, X.-Q., Yang, Q.-S.: A general solution for one dimensional chemo-mechanical coupled hydrogel rod. *Acta Mech. Sin.* **34**, 392–399 (2017)
- Liu, H.G., Bian, K., Xiong, K.: Large nonlinear deflection behavior of IPMC actuators analyzed with an electromechanical model. *Acta Mech. Sin.* **35**, 992–1000 (2019)
- Pelrine, R., Kornbluh, R., Pei, Q.B., et al.: High-speed electrically actuated elastomers with strain greater than 100%. *Science* **287**, 836–839 (2000)
- Bar-Cohen, Y., Pelrine, R., Sommer-Larsen, P., et al.: Applications of dielectric elastomer actuators. In: *Smart Structures and Materials 2001: Electroactive Polymer Actuators and Devices* (2001)
- Cao, X., Zhang, M., Zhang, Z., et al.: Review of soft linear actuator and the design of a dielectric elastomer linear actuator. *Acta Mech. Solida Sin.* **32**, 566–579 (2019)
- Moretti, G., Rosati Papini, G.P., Daniele, L., et al.: Modelling and testing of a wave energy converter based on dielectric elastomer generators. *Proc. Math. Phys. Eng. Sci.* **475**, 20180566 (2019)
- Huang, B., Li, M., Mei, T., et al.: Wearable stretch sensors for motion measurement of the wrist joint based on dielectric elastomers. *Sensor* **17**, 2708 (2017)
- Chen, Y., Zhao, H., Mao, J., et al.: Controlled flight of a micro-robot powered by soft artificial muscles. *Nature* **575**, 324–329 (2019)
- Carpi, F., Frediani, G., Turco, S., et al.: Bioinspired tunable lens with muscle-like electroactive elastomers. *Adv. Funct. Mater.* **21**, 4152–4158 (2011)
- Li, J.R., Wang, Y., Liu, L.W., et al.: A biomimetic soft lens controlled by electrooculographic signal. *Adv. Funct. Mater.* **29**, 1903762 (2019)
- Duduta, M., Berlinger, F., Nagpal, R., et al.: Tunable multi-modal locomotion in soft dielectric elastomer robots. *IEEE Robot. Autom. Lett.* **5**, 3868–3875 (2020)
- Koh, S.J.A., Zhao, X., Suo, Z.: Maximal energy that can be converted by a dielectric elastomer generator. *Appl. Phys. Lett.* **94**, 262902 (2009)
- Zhao, X.H., Suo, Z.G.: Method to analyze electromechanical stability of dielectric elastomers. *Appl. Phys. Lett.* **91**, 061921 (2007)
- Zhao, X., Suo, Z.: Electrostriction in elastic dielectrics undergoing large deformation. *J. Appl. Phys.* **104**, 123530 (2008)
- He, T., Zhao, X., Suo, Z.: Dielectric elastomer membranes undergoing inhomogeneous deformation. *J. Appl. Phys.* **106**, 083522 (2009)
- Li, B., Liu, L., Suo, Z.: Extension limit, polarization saturation, and snap-through instability of dielectric elastomers. *Int. J. Smart Nano Mater.* **2**, 59–67 (2011)
- Liu, L., Liu, Y., Luo, X., et al.: Electromechanical instability and snap-through instability of dielectric elastomers undergoing polarization saturation. *Mech. Mater.* **55**, 60–72 (2012)
- Michel, S., Zhang, X.Q., Wissler, M., et al.: A comparison between silicone and acrylic elastomers as dielectric materials in electroactive polymer actuators. *Polym. Int.* **59**, 391–399 (2009)
- Jean-Mistral, C., Sylvestre, A., Basrour, S., et al.: Dielectric properties of polyacrylate thick films used in sensors and actuators. *Smart Mater. Struct.* **19**, 075019 (2010)
- Sheng, J., Chen, H., Li, B., et al.: Temperature dependence of the dielectric constant of acrylic dielectric elastomer. *Appl. Phys. A* **110**, 511–515 (2012)
- Sheng, J., Chen, H., Li, B., et al.: Influence of the temperature and deformation-dependent dielectric constant on the stability of dielectric elastomers. *J. Appl. Polym. Sci.* **128**, 2402–2407 (2013)
- Sheng, J., Chen, H., Liu, L., et al.: Temperature effects on the dynamic response of viscoelastic dielectric elastomer. *Theor. Appl. Mech. Lett.* **3**, 054005 (2013)

26. Liu, L., Liu, Y., Yu, K., et al.: Thermoelectromechanical stability of dielectric elastomers undergoing temperature variation. *Mech. Mater.* **72**, 33–45 (2014)
27. Liu, L., Liu, Y., Li, B., et al.: Thermo-electro-mechanical instability of dielectric elastomers. *Smart Mater. Struct.* **20**, 075004 (2011)
28. Suo, Z.: Theory of dielectric elastomers. *Acta Mech. Solida Sin.* **23**, 549–578 (2010)
29. Gent, A.N.: A new constitutive relation for rubber. *Rubber Chem. Technol.* **69**, 59–61 (1996)
30. Horgan, C.O., Saccomandi, G.: Phenomenological hyperelastic strain-stiffening constitutive models for rubber. *Rubber Chem. Technol.* **79**, 152–169 (2006)
31. Li, B., Chen, H., Qiang, J., et al.: Effect of mechanical pre-stretch on the stabilization of dielectric elastomer actuation. *J. Phys. D* **44**, 155301 (2011)
32. Lv, X., Liu, L., Liu, Y., et al.: Dynamic performance of dielectric elastomer balloon incorporating stiffening and damping effect. *Smart Mater. Struct.* **27**, 105036 (2018)
33. Lu, T., Huang, J., Jordi, C., et al.: Dielectric elastomer actuators under equal-biaxial forces, uniaxial forces, and uniaxial constraint of stiff fibers. *Soft Matter* **8**, 6167 (2012)